Published online 21 May 2018 *Nucleic Acids Research, 2018, Vol. 46, No. 12* **6129–6139**
doi: 10.1093/nar/gky404

MPK-1/ERK pathway regulates DNA damage response during development through DAF-16/FOXO

Julien N. Bianco[1,2] and Björn Schumacher[1,2,*]

[1]Institute for Genome Stability in Ageing and Disease, Medical Faculty, University of Cologne, Joseph-Stelzmann-Strasse 26, 50931 Cologne, Germany and [2]Cologne Excellence Cluster for Cellular Stress Responses in Ageing-Associated Diseases (CECAD) and Center for Molecular Medicine (CMMC), University of Cologne, Joseph-Stelzmann-Strasse 26, 50931 Cologne, Germany

Received December 08, 2017; Revised April 26, 2018; Editorial Decision April 30, 2018; Accepted May 01, 2018

ABSTRACT

Ultraviolet (UV) induces distorting lesions to the DNA that can lead to stalling of the RNA polymerase II (RNAP II) and that are removed by transcription-coupled nucleotide excision repair (TC-NER). In humans, mutations in the TC-NER genes *CSA* and *CSB* lead to severe postnatal developmental defects in Cockayne syndrome patients. In *Caenorhabditis elegans*, mutations in the TC-NER genes *csa-1* and *csb-1*, lead to developmental growth arrest upon UV treatment. We conducted a genetic suppressor screen in the nematode to identify mutations that could suppress the developmental defects in *csb-1* mutants. We found that mutations in the ERK1/2 MAP kinase *mpk-1* alleviate the developmental retardation in TC-NER mutants, while constitutive activation of the RAS-MAPK pathway exacerbates the DNA damage-induced growth arrest. We show that MPK-1 act via insulin/insulin-like signaling pathway and regulates the FOXO transcription factor DAF-16 to mediate the developmental DNA damage response.

INTRODUCTION

Nucleotide excision repair (NER) removes helix-distorting lesions such as ultraviolet (UV)-induced cyclobutane pyrimidine dimers (CPDs) and pyrimidine 6–4 pyrimidone photoproducts (6–4PPs). Congenital defects in NER give rise to skin cancer susceptibility, developmental failure and premature aging with complex and yet incompletely understood genotype–phenotype correlation (1). NER is initiated by global genome (GG-) NER throughout the genome or by transcription-coupled (TC-) NER when lesions block RNA polymerase II (RNAPII) elongation. GG-NER defects are primarily linked to skin cancer predisposition in Xeroderma pigmentosum (XP) patients, while TC-NER defects lead to Cockayne syndrome (CS) that is characterized by severe postnatal developmental retardation followed by cachexia, neuronal degeneration, loss of retinal cells and premature death typically between the age of 12 and 16. Mutations in *CSA* and *CSB* in most cases lead to the classical CS type I, and in some cases to the more severe CS type II, cerebro-oculo-facio-skeletal syndrome (COFS) and to UV hypersensitivity syndrome (UVSS) (2). The causal relationship between the distinct mutations in *CSA* and *CSB* and the different syndromes and severities remain obscure, especially considering the wide variability of phenotypes and their severity. TC-NER is initiated by the CSB and CSA proteins and executed through a common NER core pathway that validates the damage, locally unwinds the DNA, excises the section containing the lesion, fills the gap and ligates the remaining nick. Mutations in the core pathway can lead to XP, trichothiodystrophy, COFS and XFE progeria, and in rare cases XP in combination with CS. With the exception of UV protection to reduce skin carcinogenesis no effective intervention treatment is available for NER syndrome patients.

Given the complexity of NER phenotypes in human and in the mouse mutants carrying similar mutations we and others have recently established the nematode *Caenorhabditis elegans* as genetically traceable model for investigating the consequences of mutations in NER in a metazoan context (3–6). We previously showed that TC-NER and GG-NER exert distinct roles in repairing UV-induced DNA lesions that primarily reflect their involvement in proliferating versus post-mitotic cell types. GG-NER is important during the rapid mitotic cell divisions in early embryos and remains important for removal of UV-induced lesions in germ cells that maintain proliferative activity throughout the animals' development and adulthood. In contrast, in late embryonic and throughout larval development and during adulthood somatic tissues require TC-NER as those cell types mostly expand in size during larval development and are invariably post-mitotic in adult animals. Upon hatching, 90% of the 558 cells in L1 larvae are already terminally differentiated as only 51 blast cells will undergo additional

*To whom correspondence should be addressed. Tel: +49 221 478 84202; Fax: +49 221 478 84204; Email: bjoern.schumacher@uni-koeln.de
Disclaimer: The funders had no role in study design, data collection and analysis, decision to publish or preparation of the manuscript.

cell divisions during consecutive larval stages to give rise to the 959 somatic cells of the hermaphrodite (7). Therefore, the consequences of mutations in GG-NER and TC-NER result in intriguing parallels to the human pathologies: TC-NER defects impair developmental growth and lead to deterioration of adult tissues, while GG-NER defects lead to genome instability in proliferating cell types, which in human underlies cancer development (8).

We previously showed that developing larvae induce the FOXO transcription factor DAF-16 upon UV-induced DNA damage. DAF-16 is negatively regulated by insulin/insulin-like signaling (IIS). Active IIS leads to phosphorylation and consequent cytosolic sequestration of DAF-16 (9,10). Upon IIS inactivation hypophosphorylated DAF-16 enters the nucleus and induces a stress response program in developing and aging animals thus promoting longevity (11). Upon DNA damage constitutive activation of DAF-16 induces the expression of developmental growth genes through the GATA transcription factor EGL-27 and thereby antagonizes the UV-induced developmental arrest even when DNA lesions could not be removed in NER mutants (5). Interestingly, we showed that DAF-16 exerts a specific growth promoting function when responding to UV-induced DNA damage, while under starvation conditions DAF-16 also responds but then represses the same developmental growth genes (5). It has remained unknown how DAF-16 is activated upon DNA damage. Similarly, how transcription blocking lesions are sensed and their presence is signaled has not been shown. These questions are important because most studies on the DNA damage response (DDR) have focused on proliferative cell types and defined DNA damage checkpoints. However, those checkpoint mechanisms are dispensable in post-mitotic tissues and operate distinct from the IIS-DAF-16 response to transcription-blocking lesions. Moreover, a dampened IIS, consistent with DAF-16 activation, has been observed in NER deficient progeroid mice, while the mechanism of the IIS dampening has remained elusive (12–14).

To define mechanisms that could overcome the developmental retardation we performed a genetic suppressor screen of *csb-1* mutants exposed to UV irradiation. We identified a mutation in the *mpk-1* gene encoding the ortholog of the ERK1/2 mitogen activated protein kinase (MAPK). We showed that an *mpk-1* mutation alleviates developmental arrest of *csb-1* and *csa-1* as well as of completely NER defective *xpa-1* mutants. In contrast, JNK-1 or PMK-1, respectively, orthologs of the MAPKs JNK and p38, were not involved. The ability of *mpk-1* mutants to boost UV resistance depended on the FOXO transcription factor *daf-16*. We show that DAF-16 activity is elevated in *mpk-1* mutants consistent with MPK-1 signaling negatively regulating DAF-16.

MATERIALS AND METHODS

Strains

All strains were cultured according to standard conditions (15). Strains used were N2 (Bristol; wild-type), RB1801 csb-1(ok2335), BJS737 mpk-1(sbj10), BJS367 mpk-1(sbj10);csb-1(ok2335), SD939 mpk-1(ga111);unc-79(e1068), BJS370 mpk-1(ga111);unc-79(e1068);csb-1(ok2335), FX04539 csa-1(tm4539), BJS449 csa-1(tm4539);mpk-1(ga111);unc-79(e1068), RB864 xpa-1(ok698), BJS457 xpa-1(ok698);mpk-1(ga111);unc-79(e1068), CF1038 daf-16(mu86), BJS593 daf-16(mu86);csb-1(ok2335), BJS400 mpk-1(ga111);unc-79(e1068);daf-16(mu86), BJS595 daf-16(mu86);mpk-1(ga111);unc-79(e1068);csb-1(ok2335), VC8 jnk-1(gk7), BJS428 jnk-1(gk7);csb-1(ok2335), BJS580 mpk-1(ga111);unc-79(e1068);jnk-1(gk7), BJS581 mpk-1(ga111);unc-79(e1068);jnk-1(gk7);csb-1(ok2335), KU25 pmk-1(km25), BJS430 pmk-1(km25);csb-1(ok2335), BJS729 mpk-1(ga111);unc-79(e1068);pmk-1(km25);csb-1(ok2335), SD551 let-60(ga89), BJS456 let-60(ga89);csb-1(ok2335), TG1387 lip-1(gt448), BJS418 lip-1(gt448);csb-1(ok2335), TJ356 zIs356[daf-16::GFP;rol-6]IV, BJS15 zIs356[daf-16::GFP;rol-6]IV;csb-1(ok2335), BJS526 mpk-1(ga111);unc-79(e1068);zIs356[daf-16::GFP;rol-6]IV and BJS525 mpk-1(ga111);unc-79(e1068); zIs356[daf-16::GFP;rol-6]IV;csb-1(ok2335), VC1217 egl-27(ok1670), BJS326 egl-27(ok1670);csb-1(ok2335), BJS708 egl-27(ok1670);mpk-1(ga111);unc-79(e1068), BJS709 egl-27(ok1670);mpk-1(ga111);unc-79(e1068);csb-1(ok2335).

EMS mutagenesis

csb-1 mutants worms were synchronized at L1 stage via standard hypochlorite treatment (16). Synchronized L1 worms were plated on Nematode Growth Medium (NGM) plates seeded with *Escherichia coli* OP50, grown until L4 and treated with 1 mM Ethyl methanesulfonate (EMS) in M9 buffer for 4 h at room temperature. A low dose of EMS was used because *csb-1* mutant animals showed hypersensitivity to EMS-induced DNA damage. Residual EMS was neutralized with 1 M NaOH and removed by two washes with 4 ml M9 buffer, and the worms were then plated on OP50-seeded NGM plates. Twenty-four hours later, F1 worms were synchronized at L1 stage with hypochlorite treatment, aliquoted and frozen. For screening, after egg-laying for 2–3 h F2 adults were backed up in 96-well plate liquid culture. F3 larvae were irradiated with 60 mJ/cm^2 UVB and screened for bypass developmental arrest 48 h post-irradiation. Phenotype was confirmed by using the worms from the 96-well backup plate. A total of 1200 F2 mutagenized worms were screened, 2 candidates were found to bypass *csb-1* UV sensitivity (including *mpk-1*) and 1 candidate to increase *csb-1* UV sensitivity.

Irradiation and analysis of somatic arrest

Developmental DDR was analyzed as previously described (17). Animals were synchronized at L1 stage via standard hypochlorite treatment. Arrested L1 larvae were put onto empty NGM plates and irradiated with 310 nm UVB light using Phillips UV6 bulbs in a Waldmann UV236B irradiation device or were mock-treated. (Irradiance was measured using a UVX digital radiometer and a UVX-31 probe from UVP and was generally around 0.3 mWcm^2.) Worms were washed off with M9 buffer, concentrated by centrifugation and put on NGM plates with a pre-grown OP50 *E. coli* lawn. Plates were kept at 15, 20 and 25°C for 48 or 72 h, and larval stages were determined by manual inspection under a dissecting microscope.

IlludinM sensitivity assay

Synchronized L1 larvae were obtained by hypochlorite treatment and were treated with indicated concentrations of illudinM in M9 medium with OP50 for 48 h at 20°C on a shaking platform. Each treatment was conducted in triplicate. In the non-treated samples, we used 0.25% Dimethyl sulfoxide (DMSO), the same concentration used in 10 μg/ml illudinM. IlludinM sensitivity was measured by determining the percentage of different larval stages in each treatment. IlludinM was a kind gift from Prof. Rainer Schobert (Bayreuth).

Actinomycin D and α-amanitin sensitivity assay

Synchronized L1 larvae were obtained by hypochlorite treatment and were treated with indicated concentrations of actinomycin D (SIGMA-ALDRICH A1410) or α-amanitin (SIGMA-ALDRICH A2263) in M9 medium with OP50 for 24 h at 20°C on a shaking platform. Then worms were plated and kept for 24 h at 25°C and then drug sensitivity was measured by determining the percentage of different larval stages in each treatment. For the actinomycin D experiment, in the non-treated samples, we used 1.25% DMSO, the same concentration used in 12.5 μg/ml actinomycin D.

DAF-16::GFP translocation

DAF-16::GFP localization was analyzed under the fluorescence dissecting microscope at given time points. Synchronized L1 worms obtained by egg-laying were plated onto NGM plates seeded with OP50 and incubated at 20°C. Worms were irradiated with 0, 40 or 80 mJ/cm^2 UVB and imaged 3, 5, 7 and 24 h after irradiation to visualize the cellular localization of the GFP fusion proteins.

Imaging of DAF-16::GFP transgenic animals

Imaging of live UV-irradiated DAF-16 reporter worms was done using a Leica SP8 Confocal microscope. Synchronized L1 worms derived from egg-laying were plated onto NGM plates seeded with OP50 and incubated at 20°C. Treated worms were irradiated with 80 mJ/cm^2 UVB. Worms were imaged 24 h after irradiation to visualize the cellular localization of the GFP fusion proteins.

Measurement of adult survival

After hypochlorite-synchronization, animals were grown to young adult stage and subjected to UVB or mock treatment. Animals were subsequently plated on OP50-seeded plates and kept at 25°C. Next, ∼150 animals per strain and condition were counted and transferred to fresh OP50-seeded plates every day until day 6 of adulthood. From then on, animals were not transferred anymore and still counted every day. Dead animals were tested for touch response by poking with a platinum wire and close observation of residual pumping movements in the pharynx. Dead animals were scored and removed from the plate. We censored animals that died from internal hatching or escaped from the plate.

Statistical analyses

Student's *t*-test was used to compare the fraction of a given larval stage upon the treatment with a specific dose of UV irradiation. The *t*-test allows assessing the robustness of the effect of the genetic mutation on the larval stage, i.e. *mpk-1* and *csb-1* genetically interact and *mpk-1* genetically suppresses a *csb-1* mutation. The Fisher's exact test was used to evaluate whether the distributions of larval stages—as a whole population—are significantly different between the *mpk-1*;*csb-1* double mutants and the *csb-1* single mutants. Each category of DAF-16::GFP translocations was analyzed by two-tailed *t*-test and the difference of the entire populations by Fisher's Exact test. *P*-value from Fisher's Exact test are reported in Supplementary Table S8 and the *P*-value for all the two-tailed *t*-tests of the different mutant combinations are shown in Supplementary Tables.

RESULTS

We performed a genetic screen to identify mutants that could alleviate the developmental arrest of *csb-1* mutant *C. elegans* after UV treatment. *csb-1* mutant worms at L1 stage are highly sensitive to UV treatment and arrest somatic development (5). We scored developmental delay by counting the stages from the L1 and the consecutive L2, L3, L4 larval stages until adulthood 48 h post-UV treatment of synchronized L1 populations (5). Using EMS, we mutagenized *csb-1(ok2335)* worms and screened the F2 generation for alleviation of the UV-induced developmental arrest (Figure 1A). We isolated a mutant strain able to bypass the L1 arrest, and after outcrossing and whole genome sequencing we identified a mutation in the *mpk-1* gene (Figure 1B), and we called this new allele *sbj10*. *mpk-1(sbj10)* mutants carry a cytosine to guanine missense mutation in the sixth exon, in position 725 of the gene (position refers to the canonical isoform b), leading to a substitution from Alanine to Valine in position 242 of the protein. The *sbj10* mutation is located 78 nucleotides downstream of another previously described point mutation in *mpk-1(ga111)*. Both of the mutations are located close to the MEK binding site, suggesting a defect in activation by the upstream kinase MEK-2 (18). Both mutations (*sbj10* and *ga111*) are located in the same highly conserved region of the protein (Supplementary Figure S1).

We observed the same phenotype in both alleles: at 20 and 25°C, *mpk-1(ga111)*;*csb-1* and *mpk-1(sbj10)*;*csb-1* mutations were able to alleviate the UV sensitivity of *csb-1* mutant (Figure 1C). In contrast, there was no influence of the developmental arrest at 15°C, indicating that as similar to the *mpk-1(ga111)* allele, as previously described (18), also the *mpk-1(sbj10)* allele is thermosensitive. As the UV doses used to arrest the development of *csb-1* mutant, wild-type (WT) and *mpk-1(ga111)* worms are not affected. However, at higher UV doses, we observed that *mpk-1(ga111)* worms are less developmentally delayed compared to WT animals, indicating that MPK-1 also function during the transient developmental arrest in NER-proficient worms (Figure 1D). In contrast, unperturbed larval developmental growth in the absence of UV-induced DNA damage was not affected by the status of MPK-1.

To validate the relevance of MPK-1 activity to TC-NER, we next tested whether *mpk-1* could also suppress the de-

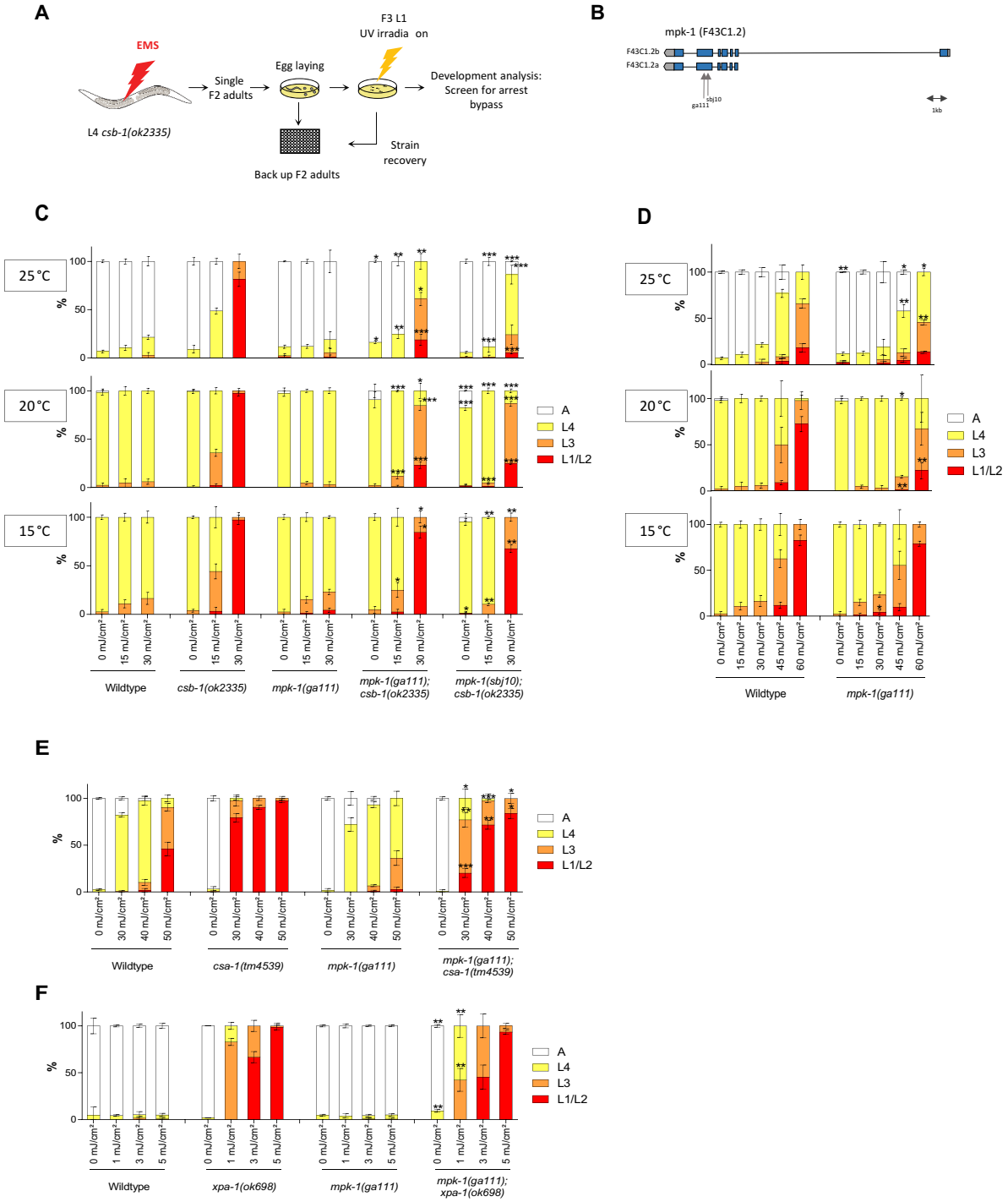

Figure 1. *mpk-1* mutations suppress UV-induced developmental growth arrest in TC-NER deficient *csb-1*, *csa-1* and in completely NER-defective *xpa-1* mutants. (**A**) *csb-1(ok2335)* worms were mutagenized with EMS (1 mM) and F2 generation synchronized by bleaching. After egg-laying for 2–3 h F2 adults were backed up in 96-well plate liquid culture. F3 larvae were irradiated with 60 mJ/cm^2 UVB and screened for bypass developmental arrest 48 h post-irradiation. Phenotype was confirmed by using the worms from the 96-well backup plate. (**B**) Representation of the genomic architecture of *mpk-1*. Blue boxes represent exons, black lines represent introns and untranslated regions are in gray. *ga111* and *sbj10* alleles are indicated. *sbj10* is a missense mutation changing Cytosine to Guanine and *ga111* is a missense mutation changing Thymine to Guanine. (**C** and **D**) L1 larvae were treated with UV and grown at 15, 20 or 25°C. Larval stages were determined 48 h post-treatment for the animals at 20 and 25°C and 72 h post-treatment for the animals at 15°C. (**E** and **F**) L1 larvae were treated with UV and grown at 25°C. Larval stages were determined 48 h post-treatment. Error bars represent standard deviation. *$P <$ 0.05, **$P < 0.01$, ***$P < 0.001$, two-tailed *t*-test comparing the fraction of each larval stage of two different mutants for the same treatment condition. *mpk-1(ga111);csb-1* and *mpk-1(sbj10);csb-1* were compared to *csb-1* in (C), *mpk-1(ga111)* was compared to WT (D), *mpk-1;csa-1* was compared to *csa-1* (E) and *mpk-1;xpa-1* to *xpa-1* (F). Statistical analysis of additional comparison and Fisher's Exact test for analyzing the distribution of larval stages see Supplementary Tables S1 and 8. Each treatment was conducted in triplicate with a minimum of 30 animals for each sample. Representative of three different experiments shown.

velopmental arrest in *csa-1* mutants. *csa-1(tm4539)* development is arrested after UV treatment as it was previously described (19), and this arrest is partially suppressed in the double mutant *mpk-1(ga111);csa-1(tm4539)* (Figure 1E). We next used *xpa-1(ok698)*, a mutation that completely abrogates NER, leading to exquisite UV sensitivity. Low doses of UV are sufficient to completely arrest development in this mutant (Figure 1F). The arrest is also significantly alleviated by *mpk-1(ga111)* (Figure 1F) suggesting that, even in the absence of any removal of UV-induced DNA lesions, abrogation of *mpk-1* could overcome the developmental growth arrest.

To test whether MPK-1 was also involved in response to other transcription blocking lesions we employed illudinM, which induces DNA lesions that require TC-NER for their removal (20) leading to strongly arrested development in TC-NER mutant animals (19). Similar to UV treatment, illudinM treatment impaired development of *csb-1* mutant worms (Figure 2A) and we observed that this delay is overcome in *mpk-1;csb-1* double mutants. Those observations indicate that MPK-1 is required for developmental arrest induced by transcription-blocking DNA lesions that remain unrepaired in *csb-1* mutants upon UV or illudinM treatment.

We next tested the consequence of transcription blockage on the *csb-1* phenotype. Treatment with actinomycin D, which intercalates the DNA and blocks the progression of RNAPs (21), led to developmental growth retardation that was exacerbated in *csb-1* mutant animals (Figure 2B). In contrast, *mpk-1* suppressed the actinomycin D sensitivity of *csb-1* mutants indicating that the developmental growth retardation emanating from transcription blockage could be overcome by dampening MPK-1 signaling. At last, we tested the sensitivity to α-amanitin, a drug that affects transcription by blocking RNAPs without inducing DNA damage. In contrast to illudinM or actinomycin D treatment, *csb-1* and *mpk-1;csb-1* mutant worms were as sensitive to α-amanitin as WT animals (Figure 2C). These data indicate that MPK-1 regulates the developmental growth arrest upon DNA lesions that block transcription.

We next wished to address whether this phenotype was specific for MPK-1/ERK signaling pathway or whether other MAPKs might also be involved. We crossed *csb-1* mutant with *jnk-1* or *pmk-1* mutant strains, the two others main MAPKs in *C. elegans* encoding orthologs for JNK and p38, respectively. In both cases, the double mutants *jnk-1*;*csb-1* and *pmk-1*;*csb-1* were as sensitive as *csb-1* mutants alone (Supplementary Figure S2a and b). *jnk-1* and *pmk-1* mutants were not able to suppress *csb-1* mutant developmental arrest, suggesting that this phenotype is specific to *mpk-1* mutations. In addition, the triple mutants *mpk-1*;*pmk-1*;*csb-1* and *mpk-1*;*jnk-1*;*csb-1* were less sensitive than the respective double mutant *pmk-1*;*csb-1* and *jnk-1*;*csb-1*, indicating that the absence of the other MAPKs does not impact the bypass of developmental arrest induced by mutant *mpk-1*. Thus, MPK-1 specifically is necessary for maintaining the arrest of TC-NER mutants after UV treatment, independently of the other MAPKs.

We next wished to address whether activation of MPK-1 signaling would show the reverse effect and exacerbate the developmental arrest upon UV-induced DNA damage. We, therefore, tested a mutant for the MPK-1 phosphatase *lip-1* (22). A *lip-1* mutation indeed enhanced the arrest of *csb-1*-mutated worms (Figure 3A). In addition, we assessed a *let-60(ga89)* mutant, that carry a constitutive active gain-of-function mutation in the retrovirus-associated DNA sequence (RAS) homolog in *C. elegans let-60* (23). The double mutant *let-60*;*csb-1* show a stronger arrest than the *csb-1* mutant alone (Figure 3B). Both *let-60(ga89)* and *lip-1(gt448)* enhance MPK-1/ERK signaling pathway activation, and lead to a stronger arrest of *csb-1* mutants after UV treatment. Thus, modulation of MPK-1/ERK signaling pathway affects the developmental arrest upon UV treatment of TC-NER mutants: activation of the pathway exacerbates the arrest, while inhibition promotes developmental growth amid DNA damage.

In order to investigate the role of MPK-1 in the response to UV-induced DNA damage during adulthood, we assessed the survival following UV treatment of young adult animals. While treatment with 150 mJ/cm^2 UVB did not affect the lifespan of WT or *mpk-1* mutant animals, *csb-1* mutants showed a significant lifespan reduction. *mpk-1*;*csb-1* double mutants showed a significant but only mildly shortened lifespan upon UV-induced DNA damage (Supplementary Figure S3). These data suggest that mutant *mpk-1* alleviates the UV-induced lifespan reduction in *csb-1* mutants. However, as the lifespan effects are mild compared to the strong suppression of the UV-induced developmental arrest, we suggest that MPK-1 predominantly regulates the DDR during developmental growth. It is conceivable that during adulthood, the role of MPK-1 in the DDR might not be as discernible as other potentially unrelated functions of MPK-1 signaling might impact the consequence of mutant *mpk-1* in the DDR as, for example, RNAi knockdown of *mpk-1* was shown to reduce lifespan (24).

Next, we wished to determine though which mechanism MPK-1 regulates the developmental growth of the animals after UV treatment. We previously established that the IIS effector transcription factor effector DAF-16 promotes developmental growth in response to UV-induced DNA damage in somatic tissues (5). We therefore assessed the involvement of DAF-16 in the MPK-1-mediated modulation of the UV-induced developmental arrest in TC-NER mutants. We used DAF-16::GFP strain in order to measure the nuclear *trans*-localization that is indicative of activation of DAF-16 (5,25). Under unperturbed condition, such as in the absence of UV irradiation, DAF-16::GFP is entirely cytosolic throughout development (5,25) (Figure 4A). In contrast, upon UV treatment DAF-16::GFP localizes to the nucleus and promotes developmental growth (5). UV-treated L1 *csb-1* mutant larvae showed nuclear localization of DAF-16::GFP (Figure 4A and for illustration of the scored categories Figure 4B) as it was previously described (5). Interestingly, at 80 mJ/cm^2 irradiation, DAF-16::GFP showed elevated nuclear localization in *mpk-1* mutants following UV treatment (Figure 4A). *mpk-1*;*csb-1* double mutants displayed a further and more sustained increase in DAF-16::GFP nuclear localization when compared to *csb-1* mutants alone (Figure 4A). These data indicate that MPK-1 negatively regulates the DNA damage-induced DAF-16 nuclear translocation upon UV treatment, both in WT and in the *csb-1* mutant background. Considering that DAF-

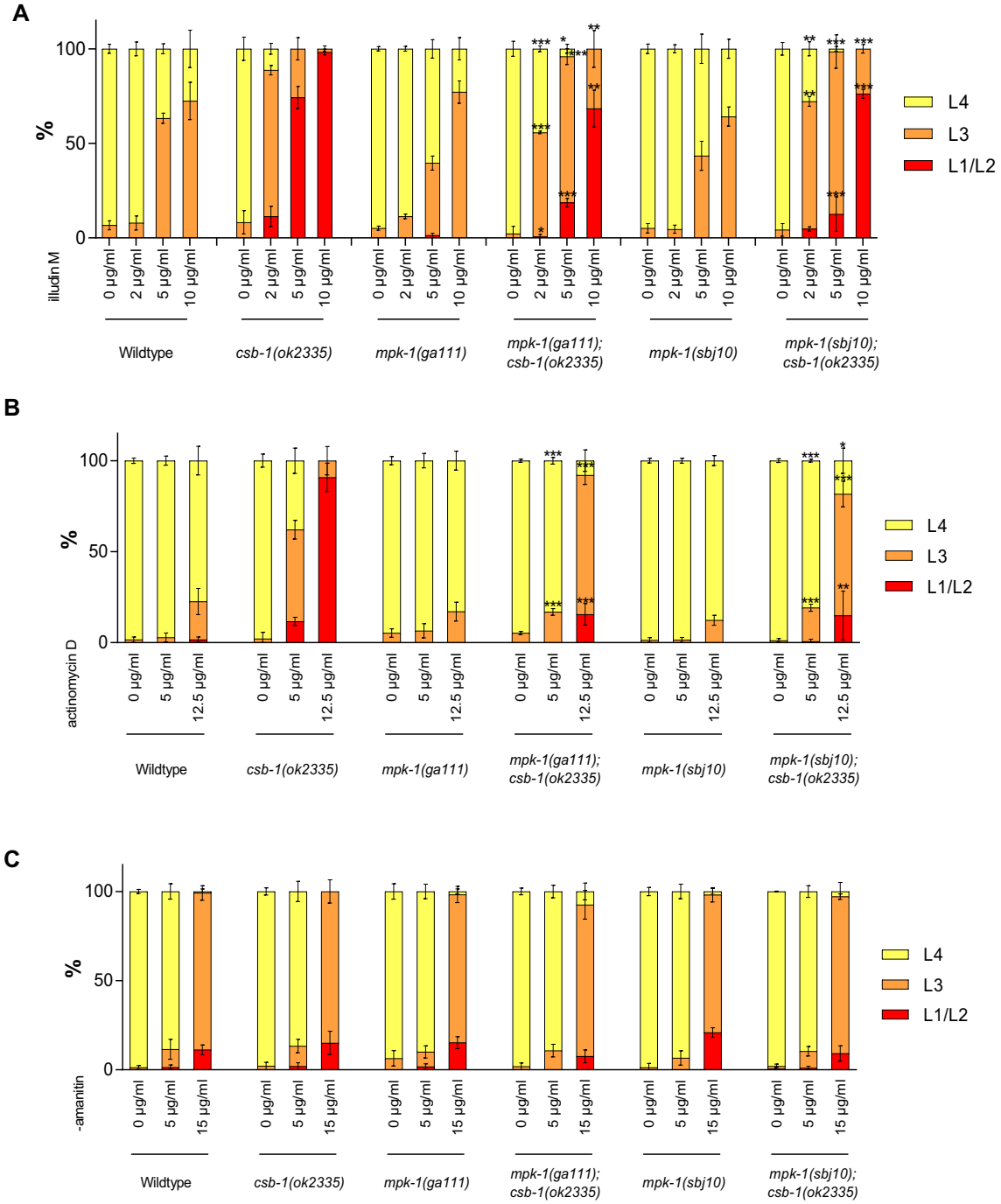

Figure 2. *mpk-1* mutation suppress *csb-1* mutant sensitivity to transcription blocking lesions. (**A**) L1 larvae were treated 48 h with different concentrations of illudinM, in liquid culture, then plated and larval stages were determined immediately. (**B**) L1 larvae were treated 24 h with different concentrations of actinomycin D, in liquid culture, then plated and larval stages were determined 24 h later at 25°C. (**C**) L1 larvae were treated 24 h with different concentrations of α-amanitin, in liquid culture, then plated and larval stages were determined 24 h later at 25°C. Error bars represent standard deviation. $*P < 0.05$, $**P < 0.01$, $***P < 0.001$, two-tailed *t*-test comparing the fraction of each larval stage of two different mutants for the same treatment condition. *mpk-1(ga111);csb-1* and *mpk-1(sbj10);csb-1 were compared to csb-1*. Statistical analysis of additional comparison and Fisher's Exact test for analyzing the distribution of larval stages see Supplementary Tables S2 and 8. Each treatment was conducted in triplicate with a minimum of 30 animals for each sample. Representative of three different experiments shown.

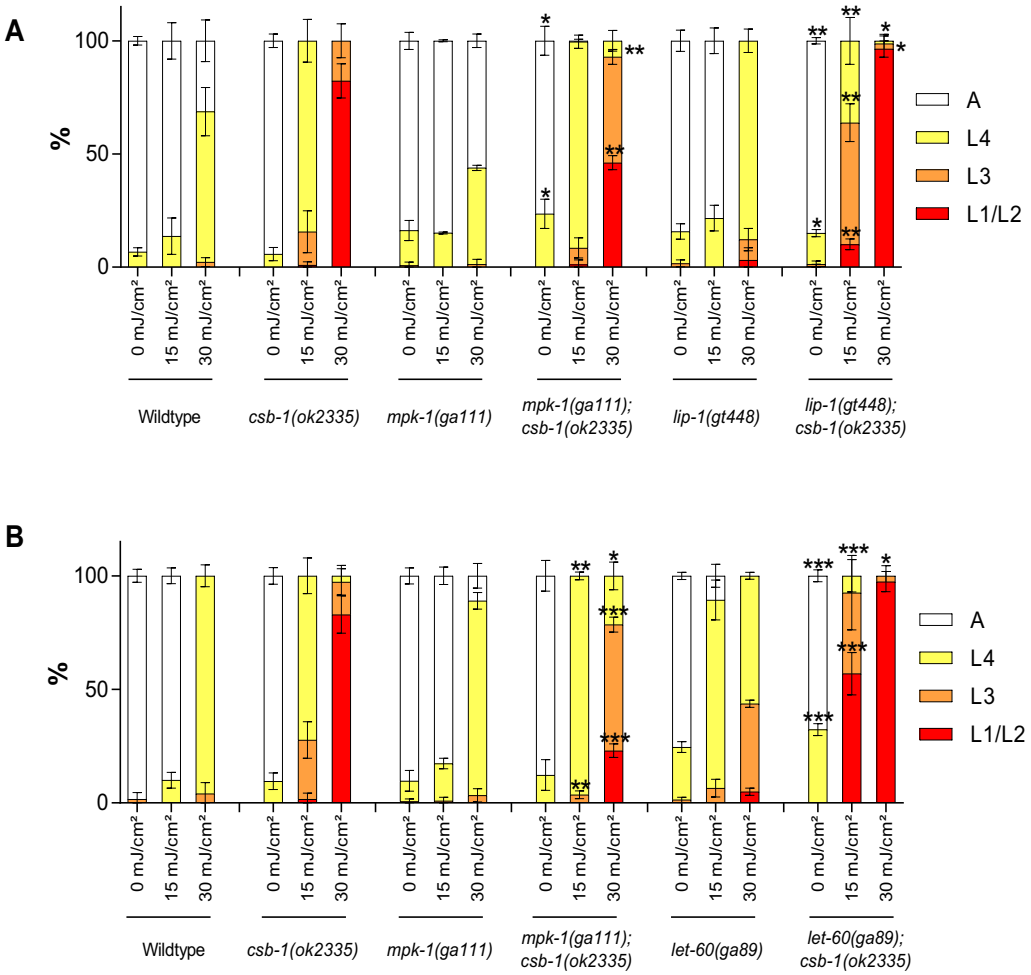

Figure 3. Modulation of MPK-1/ERK signaling pathway affects the developmental arrest upon UV treatment of csb-1. (**A** and **B**) L1 larvae were treated with UV and grown at 25°C. Larval stages were determined 48 h post-treatment. Error bars represent standard deviation. $*P < 0.05$, $**P < 0.01$, $***P < 0.001$, two-tailed *t*-test comparing the fraction of each larval stage of two different mutants for the same treatment condition. *mpk-1*;*csb-1*, *lip-1*;*csb-1* and *let-60;csb-1* were compared to *csb-1*. Statistical analysis of additional comparison and Fisher's Exact test for analyzing the distribution of larval stages see Supplementary Tables S3 and 8. Each treatment was conducted in triplicate with a minimum of 30 animals for each sample. Representative of three different experiments shown.

16 nuclear localization can promote development after UV treatment (5), we hypothesize that MPK-1 maintains UV-induced arrest of TC-NER mutants by maintaining cytosolic localization of DAF-16.

To test whether the increased DAF-16 activity was responsible for the suppression of DNA damage-induced developmental arrest, we treated *daf-16*;*mpk-1*;*csb-1* triple mutants with UV. Indeed, the suppression of the UV-induced developmental arrest in *csb-1* mutants by *mpk-1* was abrogated by a mutation in *daf-16* (Figure 4C). We also tested the involvement of the GATA transcription factor EGL-27, which we previously showed to interact with DAF-16 to promote developmental growth after UV treatment (5). Similar to the requirement of DAF-16 for UV resistance, the suppression of the UV-induced arrest of *csb-1* by *mpk-1* was also abrogated in *egl-27*;*csb-1*;*mpk-1* triple mutants (Supplementary Figure S4). Thus, DAF-16 and EGL-27 are critical effectors of the consequence of *mpk-1* on developmental arrest. Taken together, these data show that the MPK-1/ERK signaling pathway regulates the DNA damage induced developmental arrest via affecting the nuclear localization and activation of DAF-16, which together with EGL-27 confers tolerance of TC-NER deficient animals to persistent UV-induced DNA damage.

DISCUSSION

TC-NER defective CS patients suffer from severe developmental growth failure. Neither has the mechanism of the developmental defects been determined nor is there any effective intervention strategy available for CS. We therefore used the genetically traceable nematode model to identify genes that function in the developmental growth arrest and could potentially be targeted to alleviate CS phenotypes. We employed a genetic suppressor screen for the UV-induced developmental arrest of *csb-1* mutant worms and identified a mutation in the ERK1/2 MAPK *mpk-1*. We determined that constitutive activation of this pathway by constitutively active LET-60/RAS or inactivation of the LIP-1 phosphatase exacerbates DNA damage-induced develop-

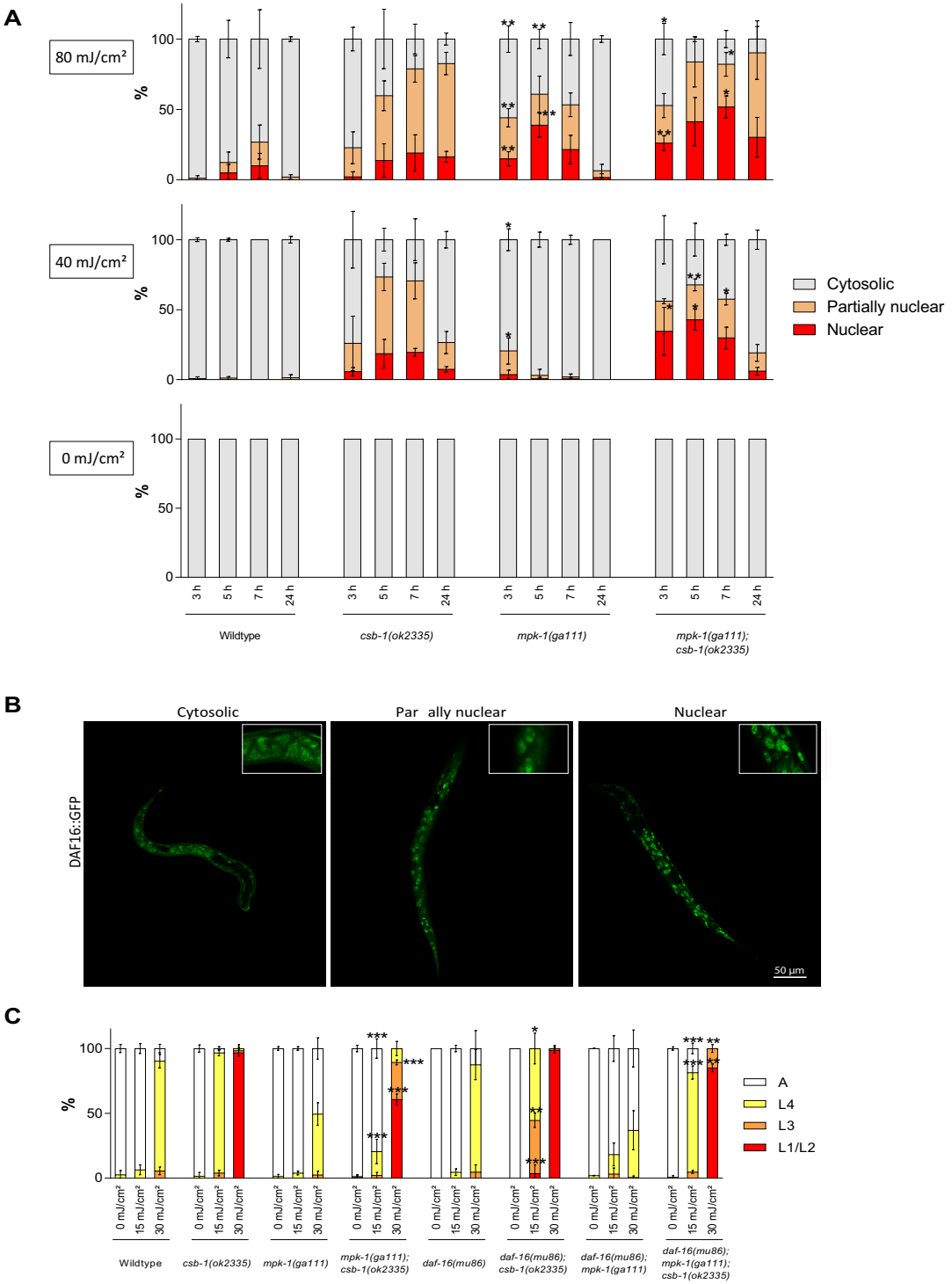

Figure 4. MPK-1 regulates DAF-16 in the developmental DDR. (**A**) DAF-16::GFP cellular localization after UV treatment in L1 larvae. WT, *csb-1*, *mpk-1* and *csb-1*;*mpk-1* strains carrying the DAF-16::GFP transgene were irradiated with 0, 40 or 80 mJ/cm^2 and kept at 20°C (average of $n = 3$ independent experiments per strain and dose is shown, 10 individuals analyzed per experiment; error bars show standard deviation). The graph shows the percentage of worms showing cytosolic, nuclear and partially nuclear DAF-16::GFP localization following UV irradiation. *$P < 0.05$, **$P < 0.01$, ***$P < 0.001$, two-tailed *t*-test comparing each type of localization of two different mutants for the same treatment condition. *mpk-1* was compared to WT and *mpk-1*;*csb-1* to *csb-1*. Statistical analysis of additional comparison and Fisher's Exact test for analyzing the distribution of larval stages see Supplementary Tables S4 and 8. (**B**) Representative pictures exemplifying the cytosolic, partially nuclear and nuclear categories of DAF-16::GFP localization, shown 24 h after UV treatment 80 mJ/cm^2 in *mpk-1(ga111)*;DAF-16::GFP c. L1 larvae were treated with UV and grown at 25°C. Larval stages were determined 48 h post-treatment. Error bars represent standard deviation. *$P < 0.05$, **$P < 0.01$, ***$P < 0.001$, two-tailed *t*-test comparing the fraction of each larval stage of two different mutants for the same treatment condition. *mpk-1*;*csb-1* and *daf-16*;*csb-1* was compared to *csb-1* and *daf-16*;*mpk-1*;*csb-1* to *mpk-1*;*csb-1*. Statistical analysis of additional comparison and Fisher's Exact test for analyzing the distribution of larval stages see Supplementary Tables S4 and 8. Each treatment was conducted in triplicate with a minimum of 30 animals for each sample. Representative of three different experiments shown.

mental arrest, while ablation of the MAPK MPK-1 could overcome the arrest even when UV-induced lesions persist in NER defective animals. Consistent with transcription-blocking lesions that destabilize elongating RNAPII (26) being the culprit of developmental retardation in NER mutants, we observed that similar to UV irradiation also illudinM and actinomycin D treatment confer a developmental delay in *csb-1* mutants that is alleviated by *mpk-1* inactivation. Therefore, the highly conserved ERK1/2 MAPK pathway regulates the developmental arrest amid unrepaired DNA lesions. Mechanistically, we determined that ablation of the MPK-1 signaling leads to elevated UV-induced activation of the FOXO transcription factor DAF-16. We previously determined that DAF-16 activity could antagonize the developmental arrest in the presence of persistent DNA lesions (5). We proposed that the induction of developmental growth and stress resistance genes by DAF-16 could elevate the capacity of post-mitotic cell types to maintain their functionality amid persistent DNA lesions. Here, we determine MPK-1 signaling as critical regulator linking the DDR to DAF-16 activity.

The highly conserved LET-60 (RAS)-MEK-2 (ERK kinase)-MPK-1 (ERK1/2) pathway has several roles in the development and homeostasis of *C. elegans*. In the soma MPK-1 is involved in vulva development (18), while in the germline MPK-1 regulates oogenesis, mitosis in germline stem cells (27), and impacts apoptosis in meiotic pachytene cells under physiological conditions as well as upon ionizing radiation (IR)-induced DNA damage (28). In mammals, MAPKs are generally activated upon different types of stimuli that include osmotic shock, DNA damaging agents, growth factors, toxins or drugs (29). The ERK1/2 signaling pathway mediates mitogenic signaling through the activation of transcription factors such as c-FOS and AP-1 (30). Constitutive activation of the ERK1/2 pathway drives proliferation in a range of cancer cells (31) and was found to be deregulated in approximately one-third of all human cancer (32). ERK1/2 signaling was also established to respond to UV irradiation (33,34) and, depending on the dose and the cell type, to induce cell cycle arrest and apoptosis (35), or transduce survival signals antagonizing stress-induced apoptosis (36). In contrast, UV treatment in T cells was shown to lead to downregulation of ERK signaling (37).

In *C. elegans* previous links have been made between IIS pathway and MPK-1. The IGF-1R homolog DAF-2 stimulates while the PTEN homolog DAF-18 inhibits MPK-1 in the regulation of vulva development, independently of DAF-16 (29). DAF-2 also regulates MPK-1 to control oogenesis (38) or apoptosis in the germline after IR (39). It has also been shown that MPK-1 controls longevity in a DAF-16-dependent manner (24). Consistent with our observations in *C. elegans,* mammalian ERK1/2 negatively regulates FOXO transcription factors. ERK1/2 phosphorylates FOXO3a, which consequently is retained in the cytoplasm, inducing its degradation thus promoting proliferation (40,41). Inhibition of ERK1/2 in mammalian cells leads to an increase of nuclear localization and activation of FOXO that in turn induces cell-cycle arrest and apoptosis (42). Wang *et al*. reported that in human cells ERK1/2 levels decreased upon UV treatment leading to nuclear localization of hypophosphorylated FOXO resulting in elevated apoptosis (40).

The versatile roles that MPK-1 plays in responding to stress as well as during development and homeostasis indicate that this pathway is activated upon distinct stimuli and that the outcome of MPK-1 activity depends on the physiological context. Indeed, mammalian ERK1/2 signaling could have differential and even antagonistic outcomes depending of the timing, duration or strength of the signal activation (30).

While the involvement of ERK1/2 signaling in the UV response has been established since several decades, here we for the first time could shed light on the consequence of the conserved MPK-1 signaling output upon UV-induced DNA damage in the context of metazoan development. Importantly, we determined that MPK-1 signaling exerts an important function in the regulation of the developmental growth delay upon transcription blocking DNA lesions, which are the culprit of TC-NER deficiencies. We established that dampening of MPK-1 signaling could confer tolerance to DNA lesions that persist in the absence of TC-NER (*csb-1* and *csa-1* mutants) and even more in completely NER-defective *xpa-1* mutants. The enhanced tolerance of transcription-blocking DNA lesions was conferred through activation of the FOXO transcription factor DAF-16, which we previously established to induce a battery of genes promoting developmental growth and stress resistance (5). Given the conserved ERK1/2 response to UV irradiation through FOXO transcription factors, this MAPK pathway might offer new opportunities to elevate tolerance to TC-NER defects and might provide intervention strategies that are still lacking for CS patients.

SUPPLEMENTARY DATA

Supplementary Data are available at NAR Online.

ACKNOWLEDGEMENTS

We thank Giorgi Berishvili for contributions to earlier phases of the project, Ashley B. Williams for support on data analysis, Arturo Bujarrabal for support for imaging and the CECAD imaging facility. Worm strains were provided by the *Caenorhabditis* Genetics Center (CGC) and the National Bioresource Project (Japan).

FUNDING

Deutsche Forschungsgemeinschaft [CECAD, SFB 829, SFB 670, KFO 286]; European Research Council (ERC Starting grant) [260383]; Marie Curie [FP7 ITN CodeAge 316354, aDDRess 316390, MARRIAGE 316964]; Bundesministerium für Bildung und Forschung (Sybacol) [FKZ0315893]; Deutsche Krebshilfe [70112899] COST action [BM1408, GENiE] to B.S.. Funding for open access charge: OpenAire [post FP7, ERC].
Conflict of interest statement. None declared.

REFERENCES

1. Cleaver,J.E., Lam,E.T. and Revet,I. (2009) Disorders of nucleotide excision repair: the genetic and molecular basis of heterogeneity. *Nat. Rev. Genet.*, **10**, 756–768.

2. Laugel,V., Dalloz,C., Durand,M., Sauvanaud,F., Kristensen,U., Vincent,M.C., Pasquier,L., Odent,S., Cormier-Daire,V., Gener,B. *et al.* (2010) Mutation update for the CSB/ERCC6 and CSA/ERCC8 genes involved in Cockayne syndrome. *Hum. Mutat.*, **31**, 113–126.
3. Lans,H., Marteijn,J.A., Schumacher,B., Hoeijmakers,J.H.J., Jansen,G. and Vermeulen,W. (2010) Involvement of global genome repair, transcription coupled repair, and chromatin remodeling in UV DNA damage response changes during development. *PLoS Genet.*, **6**, e1000941.
4. Stergiou,L., Doukoumetzidis,K., Sendoel,A. and Hengartner,M.O. (2007) The nucleotide excision repair pathway is required for UV-C-induced apoptosis in Caenorhabditis elegans. *Cell Death Differ.*, **14**, 1129–1138.
5. Mueller,M.M., Castells-Roca,L., Babu,V., Ermolaeva,M.A., Müller,R.-U., Frommolt,P., Williams,A.B., Greiss,S., Schneider,J.I., Benzing,T. *et al.* (2014) DAF-16/FOXO and EGL-27/GATA promote developmental growth in response to persistent somatic DNA damage. *Nat. Cell Biol.*, **16**, 1168–1179.
6. Wilson,D.M., Rieckher,M., Williams,A.B. and Schumacher,B. (2017) Systematic analysis of DNA crosslink repair pathways during development and aging in Caenorhabditis elegans. *Nucleic Acids Res.*, **45**, 9467–9480.
7. Sulston,J.E. and Horvitz,H.R. (1977) Post-embryonic cell lineages of the nematode, Caenorhabditis elegans. *Dev. Biol.*, **56**, 110–156.
8. Edifizi,D. and Schumacher,B. (2015) Genome instability in development and Aging: Insights from nucleotide excision repair in humans, mice, and worms. *Biomolecules*, **5**, 1855–1869.
9. Kenyon,C., Chang,J., Gensch,E., Rudner,A. and Tabtiang,R. (1993) A C. elegans mutant that lives twice as long as wild type. *Nature*, **366**, 461–464.
10. Ogg,S., Paradis,S., Gottlieb,S., Patterson,G.I., Lee,L., Tissenbaum,H.A. and Ruvkun,G. (1997) The Fork head transcription factor DAF-16 transduces insulin-like metabolic and longevity signals in C. elegans. *Nature*, **389**, 994–999.
11. Murphy,C.T., McCarroll,S.A., Bargmann,C.I., Fraser,A., Kamath,R.S., Ahringer,J., Li,H. and Kenyon,C. (2003) Genes that act downstream of DAF-16 to influence the lifespan of Caenorhabditis elegans. *Nature*, **424**, 277–283.
12. Garinis,G.A., Uittenboogaard,L.M., Stachelscheid,H., Fousteri,M., van Ijcken,W., Breit,T.M., van Steeg,H., Mullenders,L.H.F., van der Horst,G.T.J., Brüning,J.C. *et al.* (2009) Persistent transcription-blocking DNA lesions trigger somatic growth attenuation associated with longevity. *Nat. Cell Biol.*, **11**, 604–615.
13. van der Pluijm,I., Garinis,G.A., Brandt,R.M., Gorgels,T.G., Wijnhoven,S.W., Diderich,K.E., de Wit,J., Mitchell,J.R., van Oostrom,C., Beems,R. *et al.* (2006) Impaired genome maintenance suppresses the growth hormone–insulin-like growth factor 1 axis in mice with Cockayne syndrome. *PLoS Biol.*, **5**, e2.
14. Niedernhofer,L.J., Garinis,G.A., Raams,A., Lalai,A.S., Robinson,A.R., Appeldoorn,E., Odijk,H., Oostendorp,R., Ahmad,A., van Leeuwen,W. *et al.* (2006) A new progeroid syndrome reveals that genotoxic stress suppresses the somatotroph axis. *Nature*, **444**, 1038–1043.
15. Brenner,S. (1974) The genetics of Caenorhabditis elegans. *Genetics*, **77**, 71–94.
16. Porta-de-la-Riva,M., Fontrodona,L., Villanueva,A. and Ceron,J. (2012) Basic Caenorhabditis elegans methods: synchronization and observation. *J. Vis. Exp.*, **10**, e4019.
17. Rieckher,M., Bujarrabal,A., Doll,M.A., Soltanmohammadi,N. and Schumacher,B. (2017) A simple answer to complex questions: Caenorhabditis elegans as an experimental model for examining the DNA damage response and disease genes. *J. Cell. Physiol.*, **233**, 2781–2790.
18. Lackner,M.R. and Kim,S.K. (1998) Genetic analysis of the Caenorhabditis elegans MAP kinase gene mpk-1. *Genetics*, **150**, 103–117.
19. Babu,V., Hofmann,K. and Schumacher,B. (2014) A C. elegans homolog of the Cockayne syndrome complementation group A gene. *DNA Repair (Amst.)*, **24**, 57–62.
20. Jaspers,N.G., Raams,A., Kelner,M.J., Ng,J.M., Yamashita,Y.M., Takeda,S., McMorris,T.C. and Hoeijmakers,J.H. (2002) Anti-tumour compounds illudin S and Irofulven induce DNA lesions ignored by global repair and exclusively processed by transcription- and replication-coupled repair pathways. *DNA Repair (Amst.)*, **1**, 1027–1038.
21. Phillips,D.R. and Crothers,D.M. (1986) Kinetics and sequence specificity of drug-DNA interactions: an in vitro transcription assay. *Biochemistry*, **25**, 7355–7362.
22. Lee,M.-H., Hook,B., Lamont,L.B., Wickens,M. and Kimble,J. (2005) LIP-1 phosphatase controls the extent of germline proliferation in Caenorhabditis elegans. *EMBO J.*, **25**, 88–96.
23. Singh,N., Eisenmann,D.M., Kim,S.K. and Han,M. (1995) sur-2, a novel gene, functions late in the let-60 ras-mediated signaling pathway during Caenorhabditis elegans vulval induction. *Genes Dev.*, **9**, 2251–2265.
24. Okuyama,T., Inoue,H., Ookuma,S., Satoh,T., Kano,K., Honjoh,S., Hisamoto,N., Matsumoto,K. and Nishida,E. (2010) The ERK-MAPK pathway regulates longevity through SKN-1 and insulin-like signaling in Caenorhabditis elegans. *J. Biol. Chem.*, **285**, 30274–30281.
25. Henderson,S.T. and Johnson,T.E. (2001) daf-16 integrates developmental and environmental inputs to mediate aging in the nematode Caenorhabditis elegans. *Curr. Biol.*, **11**, 1975–1980.
26. Astin,J.W., O'Neil,N.J. and Kuwabara,P.E. (2008) Nucleotide excision repair and the degradation of RNA pol II by the Caenorhabditis elegans XPA and Rsp5 orthologues, RAD-3 and WWP-1. *DNA Repair (Amst.)*, **7**, 267–280.
27. Lee,M.-H., Ohmachi,M., Arur,S., Nayak,S., Francis,R., Church,D., Lambie,E. and Schedl,T. (2007) Multiple functions and dynamic activation of MPK-1 extracellular signal-regulated kinase signaling in Caenorhabditis elegans germline development. *Genetics*, **177**, 2039–2062.
28. Rutkowski,R., Dickinson,R., Stewart,G., Craig,A., Schimpl,M., Keyse,S.M. and Gartner,A. (2011) Regulation of Caenorhabditis elegans p53/CEP-1-dependent germ cell apoptosis by Ras/MAPK signaling. *PLoS Genet.*, **7**, e1002238.
29. Roux,P.P. and Blenis,J. (2004) ERK and p38 MAPK-activated protein kinases: a family of protein kinases with diverse biological functions. *Microbiol. Mol. Biol. Rev.*, **68**, 320–344.
30. Wortzel,I. and Seger,R. (2011) The ERK Cascade: Distinct functions within various subcellular organelles. *Genes Cancer*, **2**, 195–209.
31. Huntington,J.T., Shields,J.M., Der,C.J., Wyatt,C.A., Benbow,U., Slingluff,C.L. Jr, Slingluff,C.L. and Brinckerhoff,C.E. (2004) Overexpression of Collagenase 1 (MMP-1) is mediated by the ERK pathway in invasive melanoma cells. *J. Biol. Chem.*, **279**, 33168–33176.
32. Dhillon,A.S., Hagan,S., Rath,O. and Kolch,W. (2007) MAP kinase signalling pathways in cancer. *Oncogene*, **26**, 3279–3290.
33. Assefa,Z., Assefa,Z., Garmyn,M., Garmyn,M., Bouillon,R., Bouillon,R., Merlevede,W., Merlevede,W., Vandenheede,J.R., Vandenheede,J.R. *et al.* (1997) Differential stimulation of ERK and JNK activities by Ultraviolet B irradiation and epidermal growth factor in human keratinocytes. *J. Investig. Dermatol.*, **108**, 886–891.
34. Fritz,G. and Kaina,B. (1999) Activation of c-Jun N-Terminal kinase 1 by UV irradiation is inhibited by wortmannin without Affecting c-junExpression. *Mol. Cell. Biol.*, **19**, 1768–1774.
35. Tang,D., Wu,D., Hirao,A., Lahti,J.M., Liu,L., Mazza,B., Kidd,V.J., Mak,T.W. and Ingram,A.J. (2002) ERK activation mediates cell cycle arrest and apoptosis after DNA damage independently of p53. *J. Biol. Chem.*, **277**, 12710–12717.
36. Kitagawa,D., Tanemura,S., Ohata,S., Shimizu,N., Seo,J., Nishitai,G., Watanabe,T., Nakagawa,K., Kishimoto,H., Wada,T. *et al.* (2001) Activation of extracellular Signal-regulated kinase by ultraviolet is mediated through src-dependent epidermal growth factor receptor phosphorylation. *J. Biol. Chem.*, **277**, 366–371.
37. Li-Weber,M., Li-Weber,M., Treiber,M.K., Treiber,M.K., Giaisi,M., Giaisi,M., Palfi,K., Palfi,K., Stephan,N., Stephan,N. *et al.* (2005) Ultraviolet irradiation suppresses T cell activation via blocking TCR-Mediated ERK and NF- B signaling pathways. *J. Immunol.*, **175**, 2132–2143.
38. Lopez,A.L., Chen,J., Joo,H.-J., Drake,M., Shidate,M., Kseib,C. and Arur,S. (2013) DAF-2 and ERK couple nutrient availability to meiotic progression during Caenorhabditis elegans oogenesis. *Dev. Cell*, **27**, 227–240.
39. Perrin,A.J., Gunda,M., Yu,B., Yen,K., Ito,S., Forster,S., Tissenbaum,H.A. and Derry,W.B. (2013) Noncanonical control of C.

elegans germline apoptosis by the insulin/IGF-1 and Ras/MAPK signaling pathways. *Cell Death Differ.*, **20**, 97–107.
40. Wang,X., Chen,W.R., Xing,Da and Xing,D. (2011) A pathway from JNK through decreased ERK and Akt activities for FOXO3a nuclear translocation in response to UV irradiation. *J. Cell. Physiol.*, **227**, 1168–1178.
41. Yang,J.-Y., Zong,C.S., Xia,W., Yamaguchi,H., Ding,Q., Xie,X., Lang,J.-Y., Lai,C.-C., Chang,C.-J., Huang,W.-C. *et al.* (2008) ERK promotes tumorigenesis by inhibiting FOXO3a via MDM2-mediated degradation. *Nat. Cell Biol.*, **10**, 138–148.
42. Roy,S.K., Srivastava,R.K. and Shankar,S. (2010) Inhibition of PI3K/AKT and MAPK/ERK pathways causes activation of FOXO transcription factor, leading to cell cycle arrest and apoptosis in pancreatic cancer. *JMS*, **5**, 10.